Available online at www.sciencedirect.com
ScienceDirect
Journal of Sound and Vibration 318 (2008) 1180–1196
JOURNAL OF SOUND AND VIBRATION
www.elsevier.com/locate/jsvi

# Study of a self-impacting double pendulum

S. Singh*, S. Mukherjee, S. Sanghi

*Department of Mechanical Engineering, Indian Institute of Technology Delhi, New Delhi 110016, India*

Received 11 November 2007; accepted 4 May 2008
Handling Editor: L.G. Tham
Available online 13 June 2008

**Abstract**

A double pendulum with a stopper at the lower joint, as in a mammalian leg, has been studied. The impact has been modelled in a computationally efficient manner using a spring–damper in combination with a logistic function. An estimate of the coefficient of restitution of the impact based on stiffness and the damping coefficient has been developed. The response and stability of the above system have been inspected through simulations with varying coefficients of restitution. The decay rate of energy and angular momentum show dependencies unique to the case on hand.


## 1. Introduction

It has been established that torque proportional to the angle between the shank and the vertical stabilises a biped mechanism [1]. A self-impacting double pendulum is a structural component of the gait cycle of a biped with the impact being at the knee and has been studied here.

The response of a double pendulum without impacts is chaotic in nature [2]. A stopper at the lower hinge mimics the knee joint impact of a leg, as shown in Fig. 1. This self-impact may or may not curb the chaotic behaviour (intrinsic to the nonlinearity in the system), depending on the system parameters, the initial conditions and the nature of impact (elastic or otherwise).

An impact model has been used to analyse the response of a self-impacting double pendulum with varying coefficient of restitution. A methodology of modelling impact with energy losses amenable to the time domain analysis has been proposed. The method, limited only by the computational ability of the solver, assumes significance as the accuracy of solution of the nonlinear system resulting from the impact is driven by the accuracy of the impact modelling. The oscillations of the system have been studied through phase-plane plots. The decay rate of energy and angular momentum of the system from successive impacts have been tracked to study the dependence on the coefficient of restitution.

*Corresponding author.
*E-mail address:* sarabjeet.singh@yahoo.com (S. Singh).

0022-460X/$ - see front matter © 2008 Elsevier Ltd. All rights reserved.
doi:10.1016/j.jsv.2008.05.001

**Nomenclature**

| | | | |
|---|---|---|---|
| $m_1$ | mass of the upper link | $\theta_2$ | angular displacement of the lower link from vertical |
| $m_2$ | mass of the lower link | $k$ | spring stiffness |
| $l_1$ | length of the upper link | $c$ | damping coefficient |
| $l_2$ | length of the lower link | $r$ | coefficient in logistic function |
| $\theta_1$ | angular displacement of the upper link from vertical | $T_{ct}^1$ | contact force torque on the upper link |
| | | $T_{ct}^2$ | contact force torque on the lower link |

## 2. Spring–damper model of impact

### 2.1. Equations for unrestrained double pendulum

For a simple unrestrained double pendulum, the equations for kinetic energy ($T$) and potential energy ($V$) with datum at the upper hinge and generalised coordinates as ($\theta_1$, $\theta_2$, $\mathrm{d}\theta_1/\mathrm{d}t$, $\mathrm{d}\theta_2/\mathrm{d}t$) are

$$T = \frac{m_1 l_1^2 \dot{\theta}_1^2}{6} + \frac{m_2}{2}\left[\frac{l_2^2\dot{\theta}_2^2}{3} + l_1^2\dot{\theta}_1^2 + l_1 l_2 \dot{\theta}_1\dot{\theta}_2\cos(\theta_1-\theta_2)\right] \tag{1}$$

$$V = -\frac{m_1 g l_1 \cos\,\theta_1}{2} - m_2 g\left[l_1\cos\,\theta_1 + \frac{l_2\cos\,\theta_2}{2}\right]$$

$$L = T - V \tag{2}$$

$$L = \frac{m_1 l_1^2 \dot{\theta}_1^2}{6} + \frac{m_2}{2}\left[\frac{l_2^2\dot{\theta}_2^2}{3} + l_1^2\dot{\theta}_1^2 + l_1 l_2 \dot{\theta}_1\dot{\theta}_2\cos(\theta_1-\theta_2)\right] + \frac{m_1 g l_1\cos\,\theta_1}{2} + m_2 g\left[l_1\cos\theta_1 + \frac{l_2\cos\,\theta_2}{2}\right] \tag{3}$$

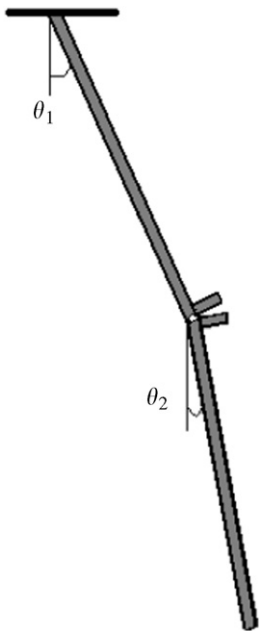


Fig. 1. Schematic of the double pendulum with a stopper at the lower hinge.

$$\frac{\mathrm{d}}{\mathrm{d}t}\left(\frac{\partial L}{\partial \dot{\theta}_i}\right) - \frac{\partial L}{\partial \theta_i} = 0 \tag{4}$$

Using the Lagrangian formulation of dynamics, we get the following equations:

$$\frac{(m_1 + 3m_2)}{3} l_1^2 \ddot{\theta}_1 + \frac{m_2 l_1 l_2 \ddot{\theta}_2 \cos(\theta_1 - \theta_2)}{2} + \frac{m_2 l_1 l_2 \dot{\theta}_2^2 \sin(\theta_1 - \theta_2)}{2} + \frac{(m_1 + 2m_2)}{2} g l_1 \sin\,\theta_1 = 0 \tag{5}$$

$$\frac{m_2 l_2^2 \ddot{\theta}_2}{3} + \frac{m_2 l_1 l_2 \ddot{\theta}_1 \cos(\theta_1 - \theta_2)}{2} - \frac{m_2 l_1 l_2 \dot{\theta}_1^2 \sin(\theta_1 - \theta_2)}{2} + \frac{m_2 g l_2 \sin\,\theta_2}{2} = 0 \tag{6}$$

### 2.2. Modelling the impact

In conventional treatise on rigid body impacts, the impact is detected by the condition of $\theta_2 > \theta_1$. The accuracy of the solution depends on the time step used in the numerical solution in the neighbourhood of the impact point. Sangwan et al. [1] described the solution to their biped mechanism as being sensitive to the time step used. However, they settled for a value low enough, such that the solution stopped varying with any further reduction in time step. Since their biped mechanism was operating in a stable periodic cycle, there were no issues in accuracy of the solution. However, for solutions of nonlinear systems operating in aperiodic regimes, error in the time of impact or the angle of impact can lead to altogether different solutions.

#### 2.2.1. Spring–damper model

Spring–damper systems have been used in nonlinear systems to examine the occurrence of chaotic motions [3,4]. Thomsen [3] analysed the dynamics of an elastically restrained inverted double pendulum (subject to follower-type non-conservative loading and linear damping) near the stationary points. Yu et al. [4] examined a similar system with linear springs (instead of torsional springs [3]) for chaos and stability. Spring–damper systems are also utilised in impact dampers for controlling high-amplitude vibrations and chaotic motion [5,6].

The interaction between two rigid bodies during the time of impact can be modelled as a spring and a damper between the bodies undergoing impact. It is imperative to ensure that the spring–damper forces come into force in the dynamic analysis only when the two bodies are infinitesimally close to each other. Chatterjee et al. [6] used a Heaviside step function in their system of equations to capture this effect. It is not possible to directly solve the equations with a step function and they substituted general solutions of the harmonic form and expanded the terms in a Fourier series.

In the double pendulum, the impact is modelled as a torsional spring and a torsional damper. The torque terms are multiplied by the Heaviside step function of the knee angle ($\theta_2 - \theta_1$):

$$\begin{aligned}&\frac{(m_1 + 3m_2)}{3} l_1^2 \ddot{\theta}_1 + \frac{m_2 l_1 l_2 \ddot{\theta}_2 \cos(\theta_1 - \theta_2)}{2} + \frac{m_2 l_1 l_2 \dot{\theta}_2^2 \sin(\theta_1 - \theta_2)}{2} + \frac{(m_1 + 2m_2)}{2} g l_1 \sin\,\theta_1 \\ &\quad + U(\theta_2 - \theta_1)(k(\theta_1 - \theta_2) + c(\dot{\theta}_1 - \dot{\theta}_2)) = 0\end{aligned} \tag{7}$$

$$\frac{m_2 l_2^2 \ddot{\theta}_2}{3} + \frac{m_2 l_1 l_2 \ddot{\theta}_1 \cos(\theta_1 - \theta_2)}{2} - \frac{m_2 l_1 l_{21} \dot{\theta}_1^2 \sin(\theta_1 - \theta_2)}{2} + \frac{m_2 g l_2 \sin\,\theta_2}{2} + U(\theta_2 - \theta_1)\big(k(\theta_2 - \theta_1) + c(\dot{\theta}_2 - \dot{\theta}_1)\big) = 0 \tag{8}$$

Since we do not have a harmonic forcing function in our system, a Fourier expansion would lead to a more complicated nonlinear system of equations with a considerable loss of accuracy. So, we chose to work with the original set of equations. The key issue here is that the Heaviside step function is not differentiable at the point of impact, when $\theta_1 = \theta_2$. To solve the set of equations in a continuous domain, an approximation of the Heaviside function (differentiable at the critical point) is required. We used the following logistic function:

$$U(\theta_2 - \theta_1) \approx \frac{1}{2}(1 + \tanh[r(\theta_2 - \theta_1)]) = \frac{1}{1 + \mathrm{e}^{-2r(\theta_2 - \theta_1)}} \tag{9}$$

As the value of $r$ is increased, the approximation becomes steeper (Fig. 2). Since we are converting a condition (of detecting impacts) into a numerical function, the value of $r$ has no bearing on the computational efficiency of the solver. Thus, for a sufficiently high value of $r \sim 10^x$, 'functional accuracy' is ensured.

To ensure better accuracy, adaptive time stepping was incorporated. The advantage of doing so is twofold. A bigger time step in regions away from the impact saves significant computation time. In the proximity of the impact point, the time interval is reduced successively such that the displacement curve is always differentiable in the impact region. With a fixed time step this may not be possible, especially in the case of sharp impact (when there is a large change in velocity before and after the impact; see Fig. 3(a)). But with an adaptive time step, the solver always ensures that the curve traverses the impact zone smoothly (Fig. 3(b)). While doing so, $\theta_2$ exceeds $\theta_1$. In a way, this behaviour is serendipitous. The collision between two rigid bodies is a finite time (though infinitesimally small) event. Bodies undergoing collision deform during the impact, much like the deformation shown in Fig. 3(b). Thus, by using this formulation of the spring–damper impact model, it is possible to accurately simulate real impacts. The values of the spring stiffness and the damping coefficient have to be determined from solid mechanics analysis of the bodies undergoing impact. The only limitation in this formulation is the computational ability of the solver. In Fig. 3(b), the impact duration is $2.68 \times 10^{-8}$ s. *Using faster computers, in principle, the impact duration can be reduced further.*

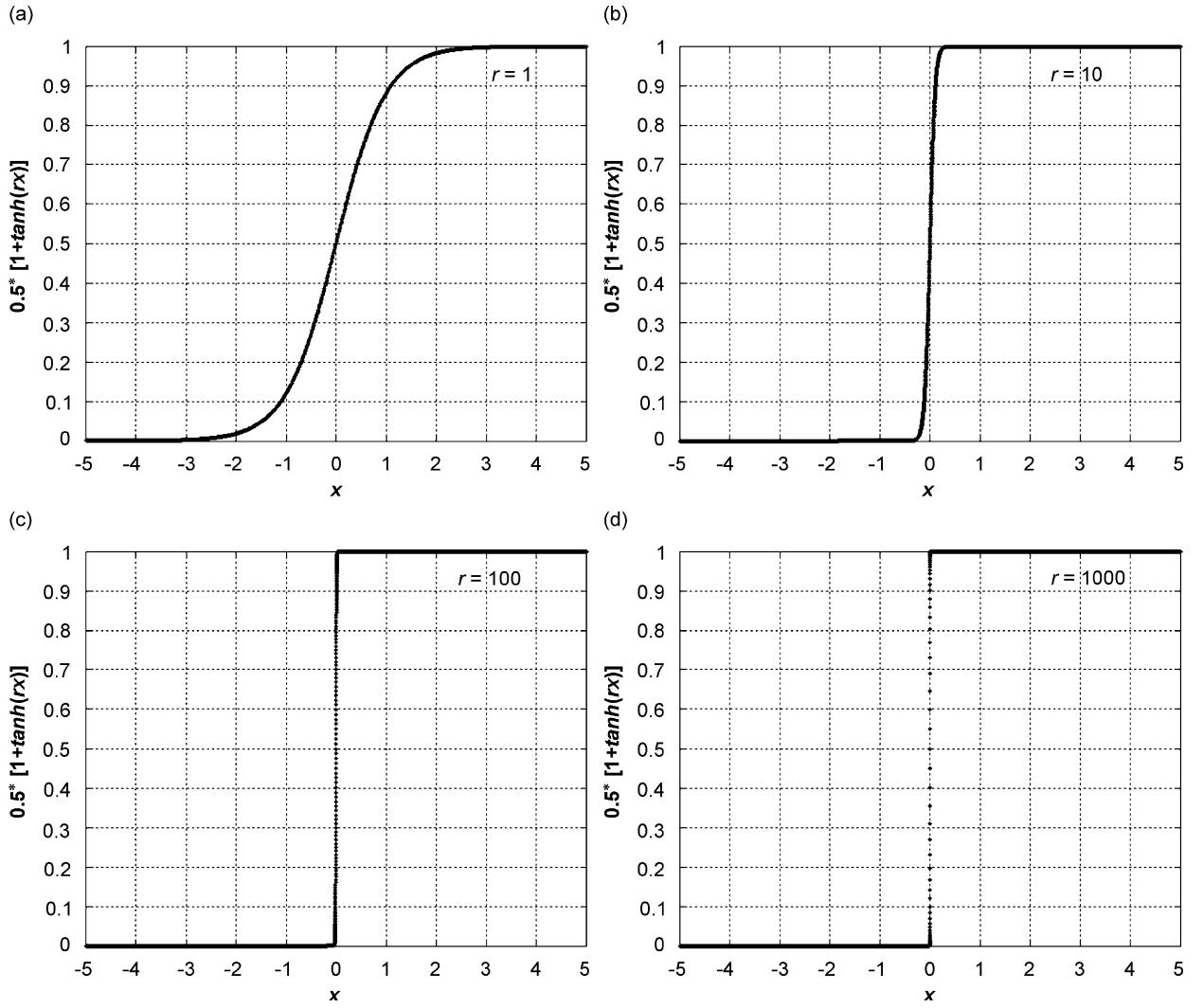


Fig. 2. Logistic function plotted for different values of $r$.

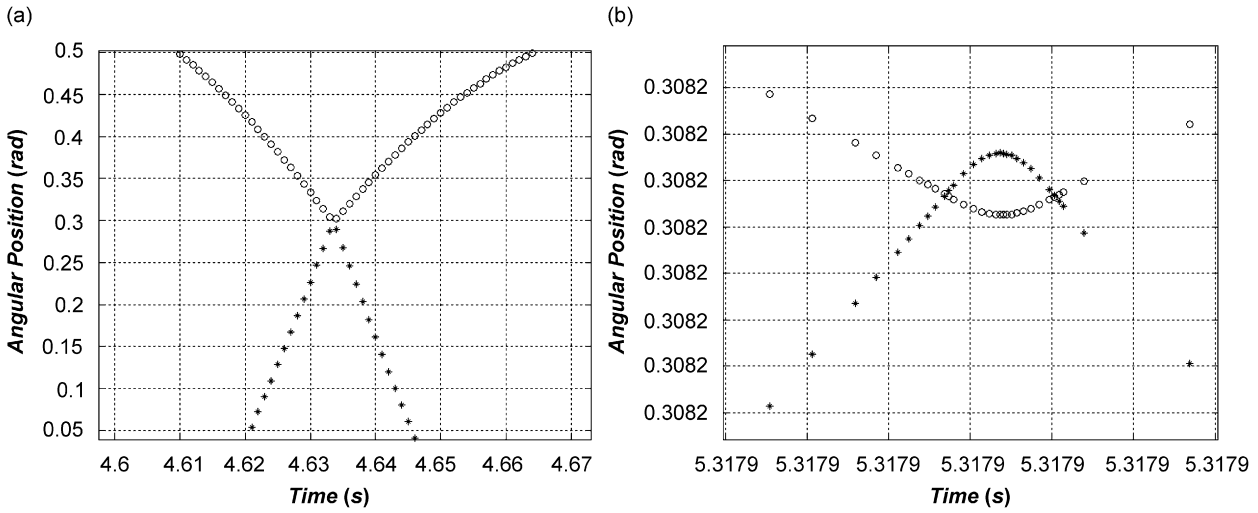


Fig. 3. Time waveform with (a) fixed time step and (b) adaptive time step. o, $\theta_1$; *,$\theta_2$.

The set of working equations thus obtained is as follows:

$$\frac{(m_1+3m_2)}{3}l_1^2\ddot{\theta}_1+\frac{m_2l_1l_2\ddot{\theta}_2\cos(\theta_1-\theta_2)}{2}+\frac{m_2l_1l_2\dot{\theta}_2^2\sin(\theta_1-\theta_2)}{2}+\left(\frac{m_1+2m_2}{2}\right)gl_1\sin\theta_1+\frac{k(\theta_1-\theta_2)+c(\dot{\theta}_1-\dot{\theta}_2)}{(1+e^{-2r(\theta_2-\theta_1)})}=0 \tag{10}$$

$$\frac{m_2l_2^2\ddot{\theta}_2}{3}+\frac{m_2l_1l_2\ddot{\theta}_1\cos(\theta_1-\theta_2)}{2}-\frac{m_2l_1l_2\dot{\theta}_1^2\sin(\theta_1-\theta_2)}{2}+\frac{m_2gl_2\sin\theta_2}{2}+\frac{k(\theta_2-\theta_1)+c(\dot{\theta}_2-\dot{\theta}_1)}{(1+e^{-2r(\theta_2-\theta_1)})}=0 \tag{11}$$

### 2.2.2. Contact force correction

Jonsson et al. [7] have highlighted the issue of contact force correction in great detail, considering all the possible transition conditions, providing simulated results for each case and have also suggested contact and non-contact conditions while modelling impact using spring and damper elements. The contact force torque on two links is given by

$$T_{ct}^1=k(\theta_2-\theta_1)+c(\dot{\theta}_2-\dot{\theta}_1) \tag{12}$$

$$T_{ct}^2=k(\theta_1-\theta_2)+c(\dot{\theta}_1-\dot{\theta}_2) \tag{13}$$

For two rigid bodies undergoing collision, the contact force in principle should always be $\geqslant 0$. If the collision is perfectly elastic, then the condition $T_{ct}^1>0$ is always satisfied in the model above. But in case there is some loss of energy involved, there can be a point where $T_{ct}^1$ crosses 0 and becomes negative. That would imply local adhesion, where although the two masses will be moving away from each other, the 'contact force' is in a direction that opposes their separation. This is an effect of the dissipation term, which always opposes the relative motion. Thus, when the spring is coming back to its relaxed position, the two terms of $T_{ct}^1$ would be opposing each other (bringing the value to 0 and then negative). To correct this situation that is not physically consistent, we need to make sure that the two masses should 'detach' completely from one another when $T_{ct}^1=0$. Physically, it implies that contact has been lost. Imposing this condition is consistent with the theory of inelastic impacts. Whenever there is an impact between two bodies, a local deformation takes place along the common normal. In the case of perfectly elastic impacts, the deformation is completely restored but in the case of inelastic impacts, some residual deformation remains when the two masses separate. To impose this condition, we use another logistic function

(approximation of the Heaviside step function of $T_{ct}^1$)

$$U(T_{ct}^1) \approx \frac{1}{2}\left[1+\tanh\left\{r(k(\theta_2-\theta_1)+c(\dot{\theta}_2-\dot{\theta}_1))\right\}\right] = \frac{1}{1+e^{-2r\{k(\theta_2-\theta_1)+c(\dot{\theta}_2-\dot{\theta}_1)\}}} \tag{14}$$

The final set of working equations that we used for simulation is given as follows:

$$\frac{(m_1+3m_2)}{3}l_1^2\ddot{\theta}_1 + \frac{m_2 l_1 l_2 \ddot{\theta}_2 \cos(\theta_1-\theta_2)}{2} + \frac{m_2 l_1 l_2 \dot{\theta}_2^2 \sin(\theta_1-\theta_2)}{2} + \frac{(m_1+2m_2)}{2} g l_1 \sin\theta_1 + \frac{k(\theta_1-\theta_2)+c(\dot{\theta}_1-\dot{\theta}_2)}{(1+e^{-2r(\theta_2-\theta_1)})(1+e^{-2r\{k(\theta_2-\theta_1)+c(\dot{\theta}_2-\dot{\theta}_1)\}})} = 0 \tag{15}$$

$$\frac{m_2 l_2^2 \ddot{\theta}_2}{3} + \frac{m_2 l_1 l_2 \ddot{\theta}_1 \cos(\theta_1-\theta_2)}{2} - \frac{m_2 l_1 l_2 \dot{\theta}_1^2 \sin(\theta_1-\theta_2)}{2} + \frac{m_2 g l_2 \sin\theta_2}{2} + \frac{k(\theta_2-\theta_1)+c(\dot{\theta}_2-\dot{\theta}_1)}{(1+e^{-2r(\theta_2-\theta_1)})(1+e^{-2r\{k(\theta_2-\theta_1)+c(\dot{\theta}_2-\dot{\theta}_1)\}})} = 0 \tag{16}$$

### 2.2.3. Coefficient of restitution

The effective coefficient of restitution during impact can be varied by changing the spring constant or the damping coefficient. The relations for coefficient of restitution stated below have been derived in the Appendix.

$$\text{Coefficient of restitution}: \quad \chi = \exp\left(\frac{-\xi}{\sqrt{1-\xi^2}}\cos^{-1}(2\xi^2-1)\right) \tag{17}$$

$$\text{Duration of impact}: \quad \delta t = \sqrt{\frac{I}{k}}\frac{\cos^{-1}(2\xi^2-1)}{\sqrt{1-\xi^2}} \tag{18}$$

$$\text{Damping ratio}: \quad \xi = \frac{c}{2\sqrt{kI}} \tag{19}$$

$$\text{Effective moment of inertia}: \quad I = \frac{(4r_m+3)m_2 l_1^2}{6(6r_l^2+6r_l+2r_m r_l^2+2)} \tag{20}$$

$$r_m = \frac{m_1}{m_2}, \quad r_l = \frac{l_1}{l_2} \tag{21}$$

Note that the duration of impact primarily depends on the value of $k$. This makes the stiffness a parameter critical for consistency. Hence, the value of $k$ is kept constant for all the simulations and the coefficient of restitution is varied through the damping coefficient $c$.

## 3. Simulation results

### 3.1. Inelastic impacts ($\chi > 0$)

The following values of the system parameters were used for the simulation:

$$m_1 = m_2 = 0.1\,\text{kg}, \quad l_1 = l_2 = 0.1\,\text{m}, \quad k = 10^{12}\,\text{N m}, \quad c \text{ has been varied}$$

For $\chi = 1$, the energy of the system is conserved (Fig. 4). The response of the system is aperiodic but follows a repeated pattern. There are 5 impacts per cycle (refer to Fig. 4(c) and (d)).

In the phase-plane plot, with $0 < \chi < 1$, a gradually collapsing set of curves is obtained. As $\chi$ is decreased (Fig. 5), the behaviour becomes more ordered, the number of impacts per cycle decreases and the variance in

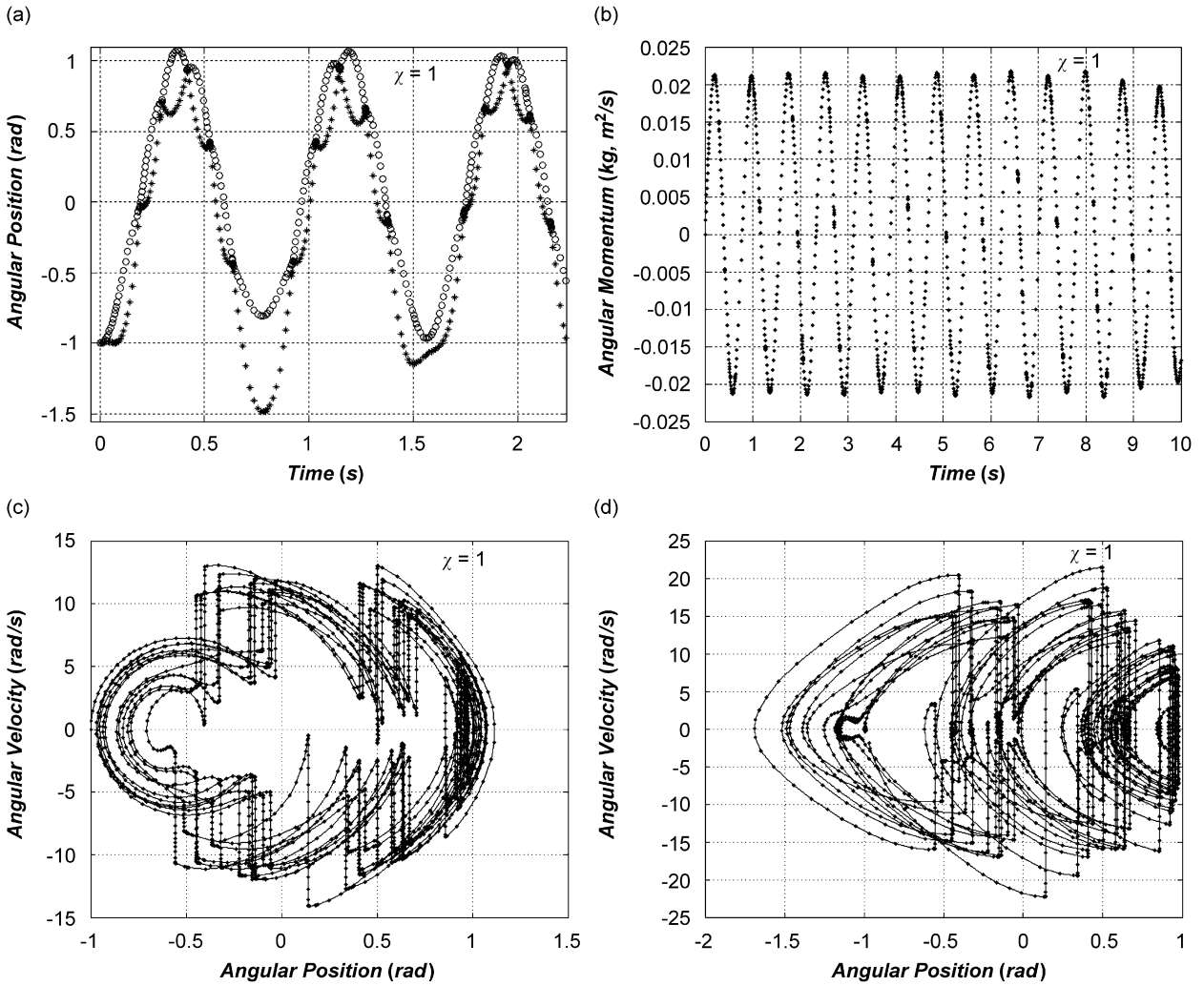


Fig. 4. (a) Time waveform. Initial condition: (−1,−1,0,0), $\chi = 1$. o, $\theta_1$; *, $\theta_2$, (b) angular momentum versus time (13 cycles), (c) phase-plane plot of $\theta_1$ ($\chi = 1$) and (d) phase-plane plot of $\theta_2$ ($\chi = 1$).

angles of impact over subsequent cycles reduces. In all cases, on the first impact, the pendulum jumps into a gradually collapsing 'attractor' after the first impact itself. The peripheral trajectory of this attractor can be termed as the limiting curve. There is a fixed-energy limiting curve (phase space) of the system, independent of the initial conditions and the coefficient of restitution. If the system starts from a point (phase space) inside the limiting curve, then it traverses the characteristic trajectory in the gradually collapsing attractor (see Fig. 5). But if the system starts from a point outside the limiting curve then it quickly jumps inside the curve after some initial impacts. We observed that while starting from outside the limiting curve, the system may not necessarily jump on the peripheral trajectory of the attractor (i.e., the limiting curve) but start on a lower trajectory close to the peripheral one.

Note that for $0.7 < \chi < 1$ (Fig. 5), there are five impacts in every cycle. For $\chi = 0.6$, there are four distinct impacts. For values of $\chi \leqslant 0.6$ there are a large number of small impacts till the two links separate completely when both link angles are 0 rad, that is, when both links are vertical.

### 3.1.1. Angular momentum

As angular momentum (about the upper hinge) is conserved during impacts, we expect that there be no jumps in the curve (see Fig. 6). For $\chi < 1$, the angular momentum varies sinusoidally with the amplitude of

successive peaks decaying exponentially (see Fig. 6). The slope of the envelope flattens as the solution progresses in time (see Fig. 7(a)). The angular momentum curve is a good indicator of the periodicity. The number of cycles of the response can be identified more easily than in the phase-plane plots (Fig. 6).

Fig. 7(b) depicts the time period ($T$) of oscillations of the pendulum plotted against time. As can be seen in the figure, the time period never attains a fixed value but flutters about a mean value. The time period, when averaged out on the asymptotic zone, is 0.738. From statistical curve fitting we found that the following function maps the decay pattern of the angular momentum:

$$H = Ae^{-(t/\alpha)^{\beta}} \sin(\omega(t) + \phi) \tag{22}$$

where $\alpha$, $\beta$ are the function parameters, $\omega$ is a function of time (Fig. 10), $\phi$ depends on the initial condition.

The angular frequency function $\omega(t)$ cannot be approximated by an explicit function. However, the averaged out value of $\omega(t)$ is best mapped by the following *exponential chirp* function:

$$\omega(t) = B - Ce^{-(t/\tau)} \tag{23}$$

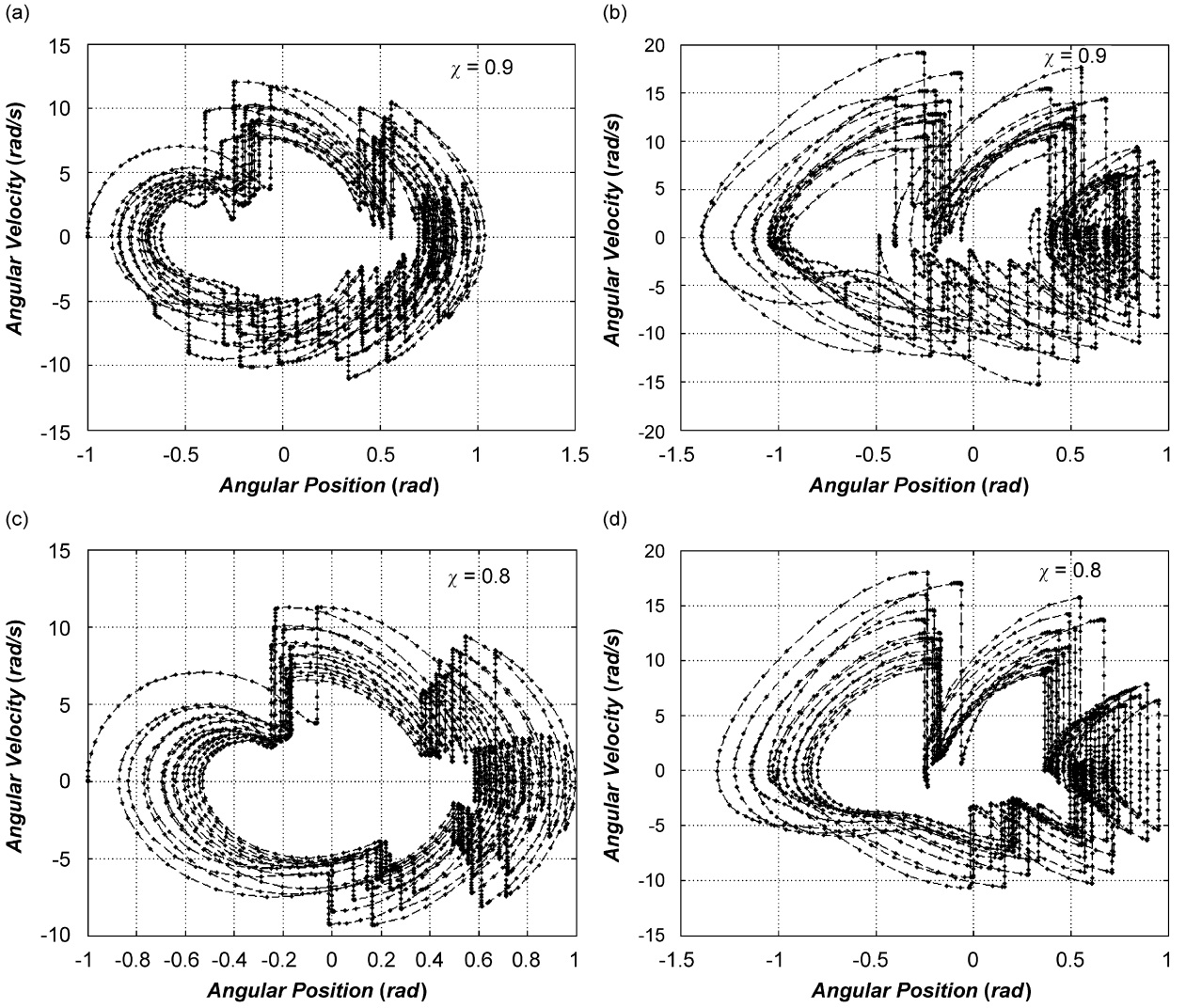


Fig. 5. Phase-plane plots of the pendulum with varying coefficient of restitution (13 cycles). Initial condition: (−1,−1,0,0). (a) $\theta_1$ ($\chi = 0.9$), (b) $\theta_2$ ($\chi = 0.9$), (c) $\theta_1$ ($\chi = 0.8$), (d) $\theta_2$ ($\chi = 0.8$), (e) $\theta_1$ ($\chi = 0.7$), (f) $\theta_2$ ($\chi = 0.7$), (g) $\theta_1$ ($\chi = 0.6$) and (h) $\theta_2$ ($\chi = 0.6$).

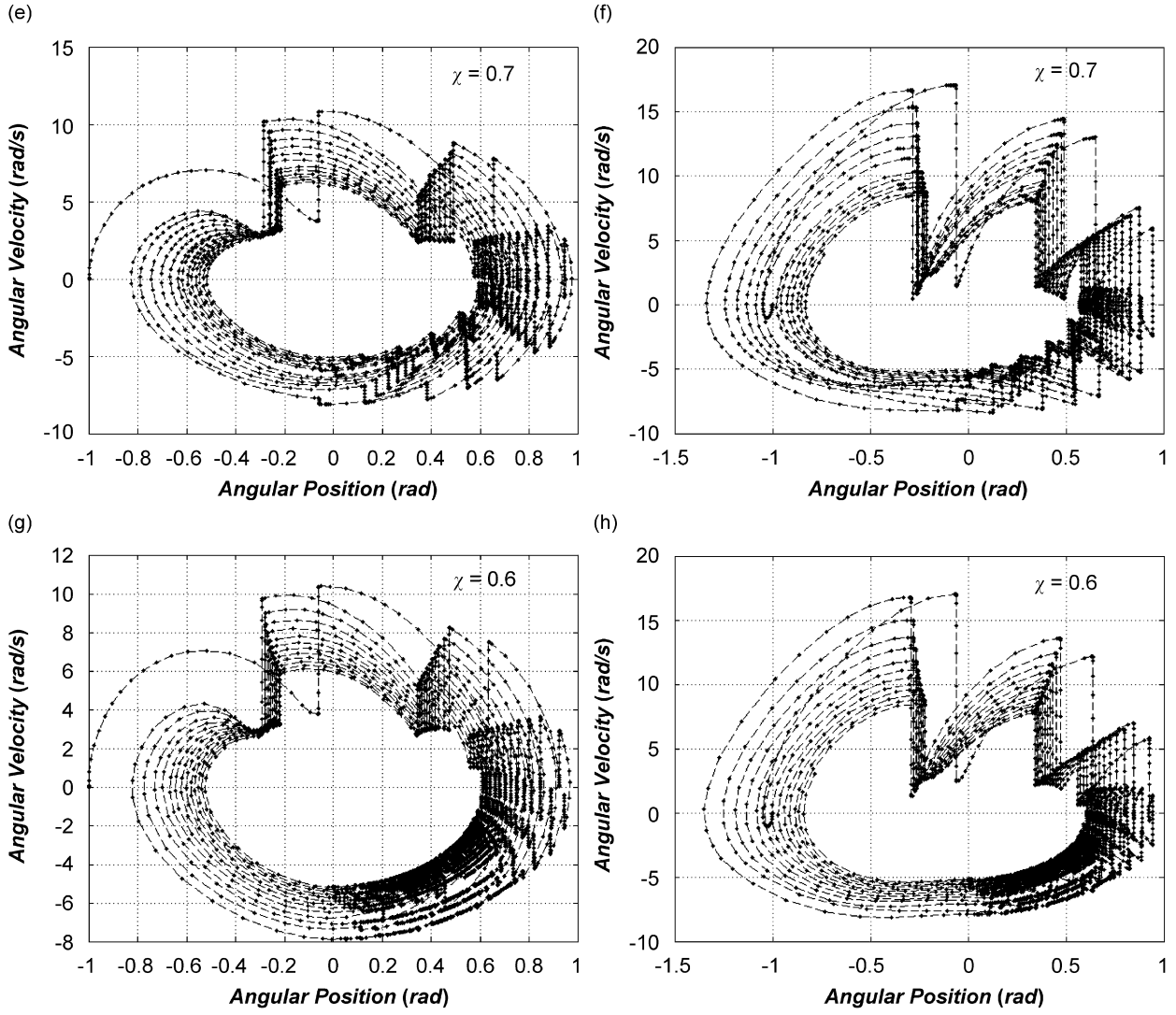


Fig. 5. (*Continued*)

There is no qualitative change in the time response of angular momentum with change in the coefficient of restitution. The envelopes of the angular momentum decay have been plotted in Fig. 8 for different values of the coefficient of restitution. It has been found that the system undergoes the same number of oscillations in a fixed time interval irrespective of the coefficient of restitution. This establishes that the time period (or frequency of oscillations) is a property of the mass and length parameters of the system only. In each case (of varying coefficient of restitution) the time period asymptotically attained a fixed (averaged out) value as in Fig. 7(b).

Although there is no qualitative change in the shape of the envelope curves (see Fig. 8), there is a quantitative change for varying values of coefficient of restitution. The parameter values of the curve fit are shown in Table 1. The $R^2$ value for all the fits is greater than 0.999, i.e., near perfect fit. Though we have only simulated till $\chi = 0$, we expect that for $0 < \chi < 0.6$, the response would be similar to those shown in Fig. 8.

The parameter values of the curve fit for angular frequency $\omega$ are shown in Table 2.

### 3.1.2. Energy

As the coefficient of restitution is reduced, the trends in the energy loss in the system behave contrary to intuition. It would be expected that the response would die down more quickly as the coefficient of restitution

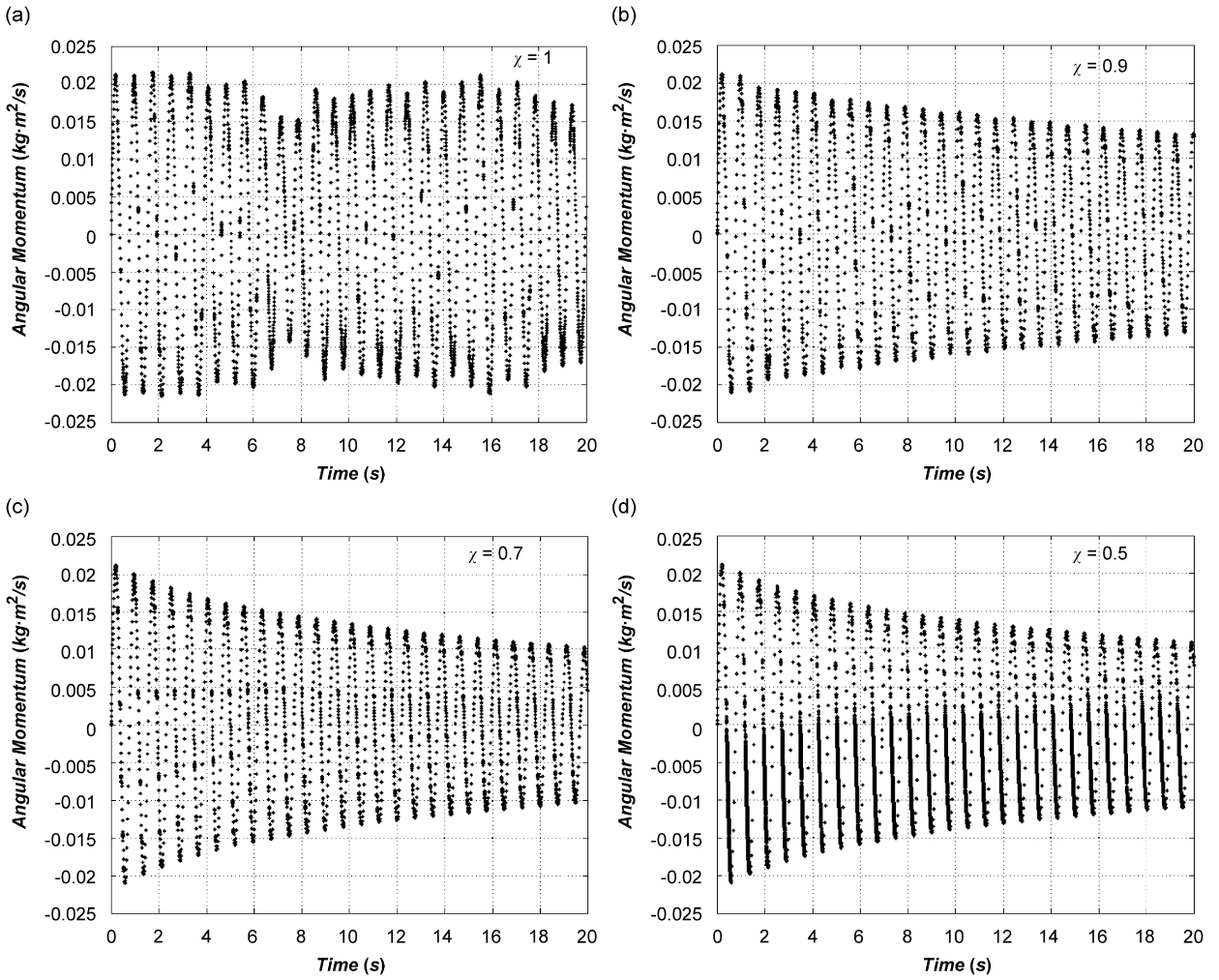


Fig. 6. Angular momentum versus time for different values of coefficient of restitution (25 cycles). Initial condition: (−1,−1,0,0).

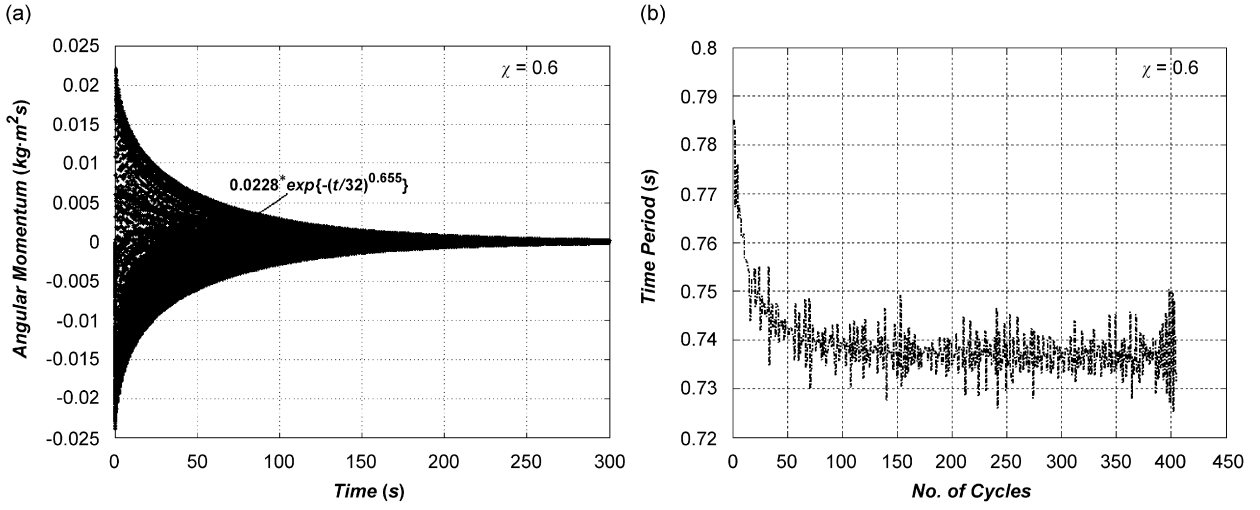


Fig. 7. (a) Angular momentum versus time and (b) periodicity versus number of cycles.

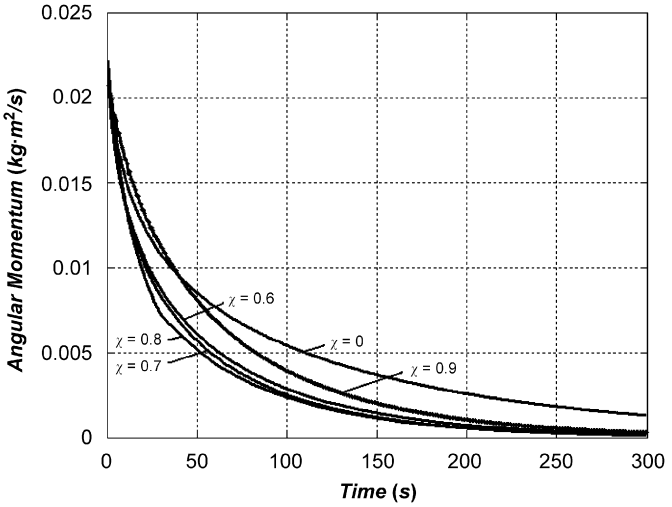


Fig. 8. Envelope of angular momentum versus time for varying coefficient of restitution.

Table 1
Parameter values of curves fit to angular momentum envelopes

| Coefficient of restitution | $A$ | $\alpha$ | $\beta$ |
|---|---|---|---|
| 0.9 | 0.02151 | 51.3 | 0.81 |
| 0.8 | 0.02574 | 21.9 | 0.59 |
| 0.7 | 0.02258 | 30.1 | 0.67 |
| 0.6 | 0.02281 | 32 | 0.655 |
| 0 | 0.02329 | 49.2 | 0.56 |

Table 2
Parameter values of curves fit to angular frequency curve

| Coefficient of restitution | $B$ | $C$ | $\tau$ |
|---|---|---|---|
| 0.9 | 8.54 | 0.448 | 24 |
| 0.8 | 8.53 | 0.491 | 12 |
| 0.7 | 8.53 | 0.449 | 14.8 |
| 0.6 | 8.52 | 0.466 | 15.5 |
| 0 | 8.51 | 0.436 | 23.5 |

is decreased. But it is observed that as the coefficient decreases (Fig. 9), the energy loss after the same time might actually decrease.

Fig. 9 shows the energy of systems after 25 cycles with varying coefficients of restitution when started at the same energy level. Counter intuitively, the figures indicate that the energy remaining in the system after 20 s decreases with increase in $\chi$ (from 0 to 0.8). This unexpected phenomenon is due to change in the number of impacts per cycle. As the coefficient of restitution increases, the number of impacts per cycle also increase, which give a higher energy loss in totality even though the energy loss per impact is less. A lower coefficient of restitution gives higher energy loss per impact but less number of impacts per cycle. For $\chi > 0.8$, the trend changes, and as expected, the decay in energy is more rapid for smaller $\chi$ (see Fig. 9(b)). Thus, there is a minima in the rate of energy decrease around $\chi = 0.8$ i.e., maximum energy loss takes place for this value of $\chi$. (Note that the curves appear jagged because the energy losses occur only at impacts but is constant otherwise.)

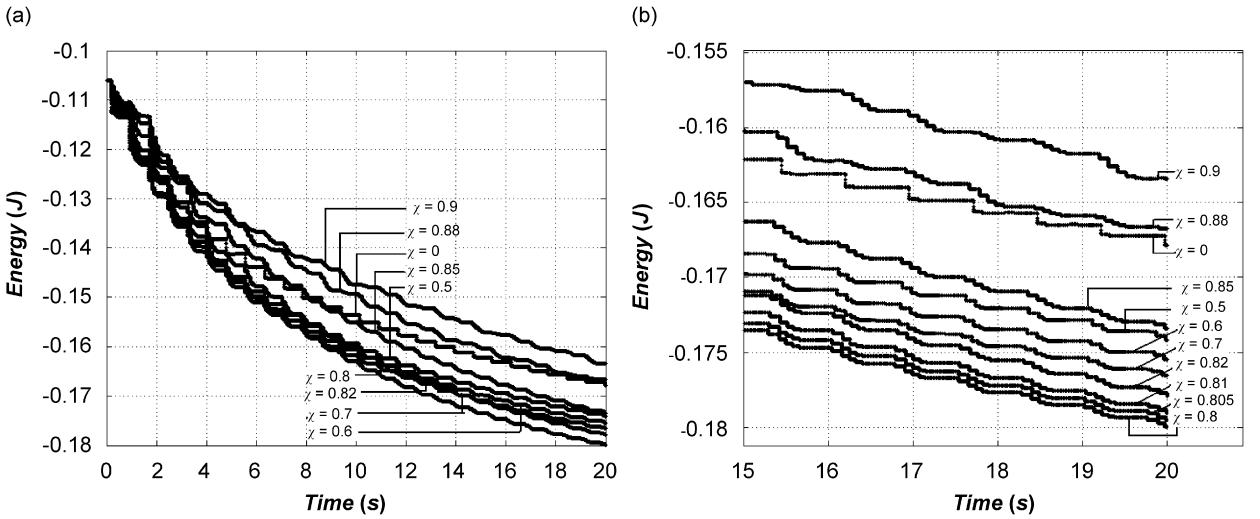


Fig. 9. (a) Energy versus time for 25 cycles. Initial condition: (−1,−1,0,0), (b) enlarged view of energy decay.

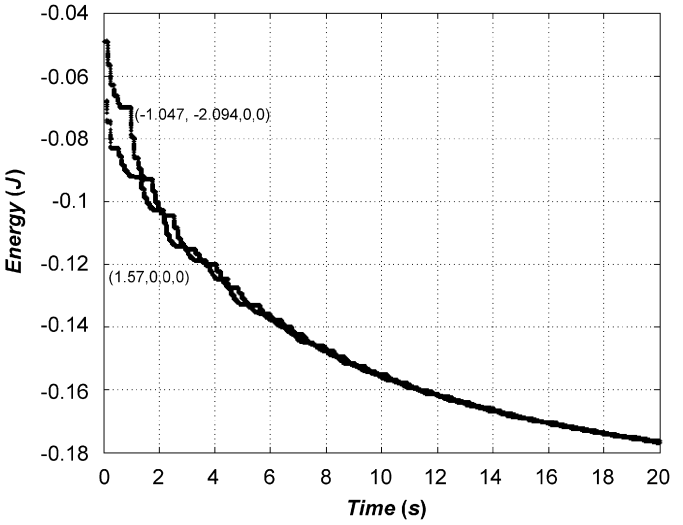


Fig. 10. Energy versus time plot for two different initial conditions with same initial energy.

Two different sets of initial conditions with the same initial energy may produce different response. This is because the angular position of the first impact and the energy lost in that impact would be different for different sets of initial conditions, even with the same initial energy (see Fig. 10). However, after a brief initial phase, the energy decay curves become coincident, i.e., the trajectories come close after an initial phase.

### 3.2. Plastic impacts ($\chi = 0$)

The case of $\chi = 0$ (plastic impacts) can be considered separately as the phase-plane plots are characterised by two impacts per cycle (see Fig. 11). In the case of idealised linear plastic impacts, the two impacting masses stick and move as a single unit after the impact. However, in the case of the double pendulum, the links separate for some time interval after the initial impact and subsequently impact again and move together as a

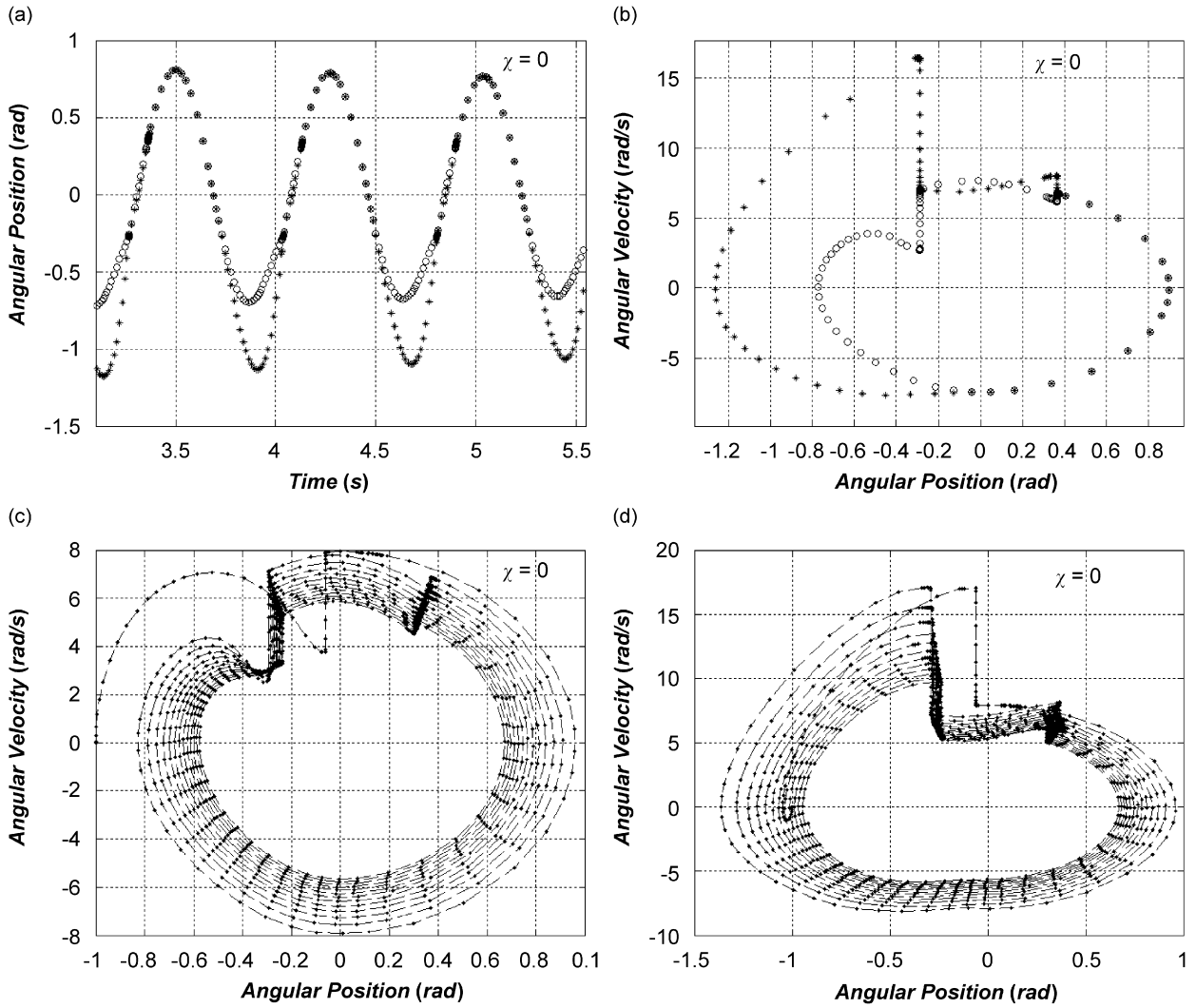


Fig. 11. (a) Time waveform. Initial condition: (−1,−1,0,0). o, $\theta_1$; *, $\theta_2$, (b) a phase-plane cycle, (c) phase-plane plot of $\theta_1$ (13 cycles) and (d) phase-plane plot of $\theta_2$ (13 cycles).

single pendulum before separating again at $\theta_{1,2} = 0$ (see Fig. 11(b)). We shall refer to the impact after which they separate as the first impact, and the one after which they stick as the second impact.

We have verified that separation is not a numerical defect, but a phenomenon consistent with intuition. The first impact takes place in the negative half of the $\theta$ domain and the second impact takes place in the positive half (Fig. 11(b)). The stopper causes impact in one direction. After the first impact, the reaction forces of the upper hinge and the lower link exert a couple (about the centre of mass) on the upper link that causes its angular acceleration to be higher than that of the lower link (which is only acted upon by the reaction force of the upper link). The net torque acts to separate the links after impact, which is observed in the simulation. The second impact takes place in the positive $\theta$ domain where the net torque attempts to separate the links in a direction that is resisted by the stopper. The two links hence end up sticking together there on.

### 3.2.1. Angular momentum

The angular momentum and angular frequency ($\omega$) of oscillations are plotted in Figs. 12 and 13, respectively.

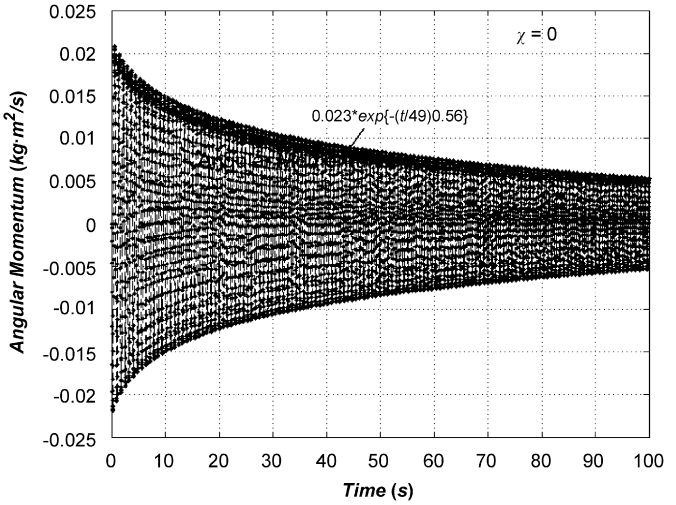


Fig. 12. Angular momentum versus time (133 cycles).

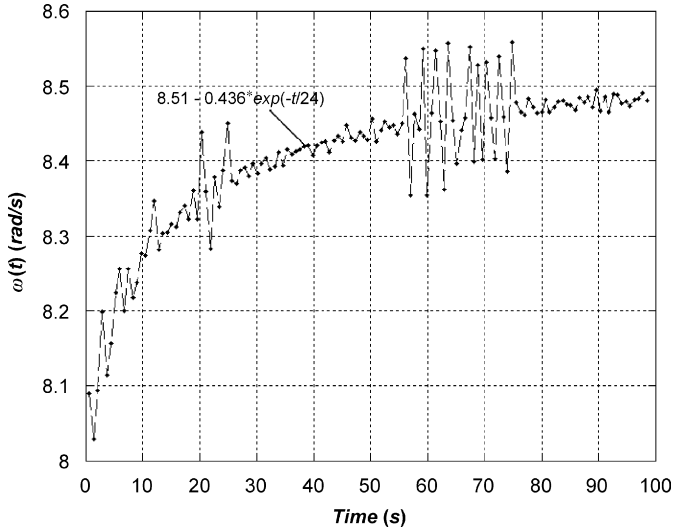


Fig. 13. Angular frequency versus time (133 cycles).

### 3.2.2. *Energy*

Energy decays in a concave curve (see Fig. 14(a)). If the energy lost per impact is plotted against the number of cycles (the energy loss takes place primarily during the first impact as shown in Fig. 14(b), so the second one can be ignored for all practical purposes), the decay has a steep slope (see Fig. 14(c)) for the initial 20 odd cycles following which the curve asymptotic approaches 0. The ratio of energy lost in successive impacts is plotted versus the number of cycles in Fig. 14(d). After being smooth initially (for 30 odd cycles), the curve becomes noisy and asymptotically approaches the value 1. The noise is expected, as the energy loss per cycle is quite small in the later cycles.

## 4. Conclusion

The impact model has been used to analyse the response of a self-impacting double pendulum with varying coefficient of restitution. A methodology of modelling impact with energy losses amenable to time domain

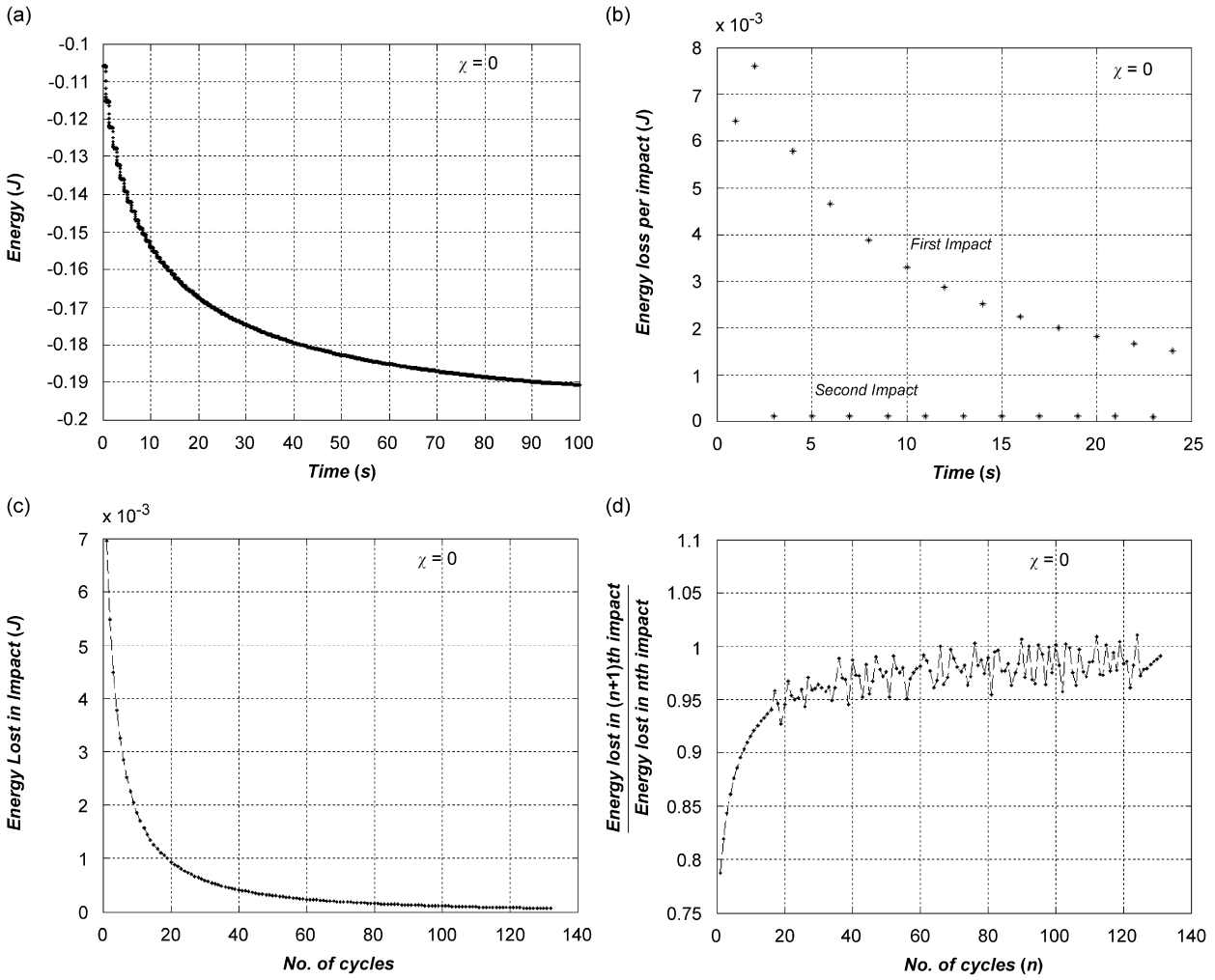


Fig. 14. (a) Energy versus time, (b) comparison of energy lost in first impact and second impact, (c) energy lost per impact versus number of cycles and (d) ratio of energy lost in successive impacts versus number of cycles.

analysis has been demonstrated. The method, limited only by the computational ability of the solver, assumes significance as the accuracy of solution of the nonlinear system resulting from the impact is driven by the accuracy of the impact modelling. A double pendulum with inelastic self-impacts at the lower hinge is shown to oscillate in a gradually collapsing (phase plane) attractor. The highest energy bound of this attractor (the limiting curve) is independent of the coefficient of restitution and the initial conditions. The (time averaged) time period of oscillations of the system approaches a unique value asymptotically, which depends only on the mass and length parameters.

The energy lost after a fixed time interval (starting from the same energy level) surprisingly increases with the coefficient of restitution in the range $\chi = 0$–$0.8$. There is an energy minima at $\chi = 0.8$, beyond which the trend reverses and as usually expected, the energy loss decreases with increase in $\chi$. The angular momentum decay rate is seen statistically to be exponential with the $R^2$ (fitness parameter) value greater than 0.999. The case of plastic impact, $\chi = 0$, is special and characterised by smooth phase-plane trajectories with two impacts that have different flavours. One of the impacts has no sticking phase at all and the separation is immediate even though it is modelled as plastic.

## Appendix

The method used in this derivation follows closely the method of calculating the coefficient of restitution in terms of spring–damper terms for liner impacts as described in Chatterjee et al. [6].

The mathematical model of impact in the double pendulum is shown in Fig. 15. The contact dynamics is represented by the following set of equations:

$$\frac{(m_1+3m_2)}{3}l_1^2\ddot{\theta}_1+\frac{m_2l_1l_2\ddot{\theta}_2\cos(\theta_1-\theta_2)}{2}+\frac{m_2l_1l_2\dot{\theta}_2^2\sin(\theta_1-\theta_2)}{2}+\frac{(m_1+2m_2)}{2}gl_1\sin\theta_1 + k(\theta_1-\theta_2)+c(\dot{\theta}_1-\dot{\theta}_2)=0 \tag{24}$$

$$\frac{m_2l_2^2\ddot{\theta}_2}{3}+\frac{m_2l_1l_2\ddot{\theta}_1\cos(\theta_1-\theta_2)}{2}-\frac{m_2l_1l_2\dot{\theta}_1^2\sin(\theta_1-\theta_2)}{2}+\frac{m_2gl_2\sin\theta_2}{2}+k(\theta_2-\theta_1)+c(\dot{\theta}_2-\dot{\theta}_1)=0 \tag{25}$$

In the presence of high impact force the gravity force terms can be neglected. Also, in the impact zone: $\theta_1-\theta_2\approx 0$, giving the following reduced equations:

$$\frac{(m_1+3m_2)}{3}l_1^2\ddot{\theta}_1+\frac{m_2l_1l_2\ddot{\theta}_2}{2}+k(\theta_1-\theta_2)+c(\dot{\theta}_1-\dot{\theta}_2)=0 \tag{26}$$

$$\frac{m_2l_2^2\ddot{\theta}_2}{3}+\frac{m_2l_1l_2\ddot{\theta}_1}{2}+k(\theta_2-\theta_1)+c(\dot{\theta}_2-\dot{\theta}_1)=0 \tag{27}$$

Putting $\phi=\theta_1-\theta_2$, the equations are further reduced to

$$I\ddot{\phi}+c\dot{\phi}+k\phi=0 \tag{28}$$

where

$$I=\frac{(4r_m+3)m_2l_1^2}{6(6r_l^2+6r_l+2r_mr_l^2+2)} \tag{29}$$

$$r_m=\frac{m_1}{m_2},\quad r_l=\frac{l_1}{l_2}$$

At the beginning of the contact phase, $t=0$, $\phi=0$, $\mathrm{d}\phi/\mathrm{d}t=-\omega$. The end of the contact phase is determined by the time at which the contact force becomes 0, i.e., $k\phi+c\mathrm{d}\phi/\mathrm{d}t=0$ or $\mathrm{d}^2\phi/\mathrm{d}t^2=0$. Conventionally, the end of the contact is determined by the time at which $\phi$ becomes 0 again. However, making the contact force 0 gives a more accurate result. At the end of the contact phase

$$t_c=\sqrt{\frac{I}{k}}\frac{\cos^{-1}(2\xi^2-1)}{\sqrt{1-\xi^2}} \tag{30}$$

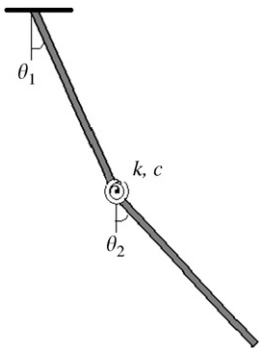


Fig. 15. Spring–damper model of self-impact in a double pendulum.

$$\dot{\phi}_c = \omega e^{\left((-\xi/\sqrt{1-\xi^2})\cos^{-1}(2\xi^2-1)\right)} \tag{31}$$

$$\xi = \frac{c}{2\sqrt{kI}} \tag{32}$$

where $t_c$ represents the duration of impact and $(d\phi/dt)_c$ is the relative velocity when the contact is lost. Thus from the definition of coefficient of restitution ($\chi$)

$$\chi = \exp\left(\frac{-\xi}{\sqrt{1-\xi^2}}\cos^{-1}(2\xi^2-1)\right) \tag{33}$$

## References

[1] V. Sangwan, A. Taneja, S. Mukherjee, Design of a robust self-excited biped walking mechanism, *Journal of Mechanism and Machine Theory* 39 (2004) 1385–1397.

[2] T. Stachowiak, T. Okada, A numerical analysis of chaos in the double pendulum, *Journal of Chaos, Solitons and Fractals* 29 (2006) 417–422.

[3] J.J. Thomsen, Chaotic dynamics of the partially follower-loaded elastic double pendulum, *Journal of Sound and Vibration* 188 (3) (1995) 385–405.

[4] P. Yu, Q. Bi, Analysis of non-linear dynamics and bifurcations of a double pendulum, *Journal of Sound and Vibration* 217 (4) (1998) 691–736.

[5] S.L.T. de Souza, I.L. Caldas, R.L. Viana, J.M. Balthazar, R.M. L.R.F. Brasil, Impact dampers for controlling chaos in systems with limited power supply, *Journal of Sound and Vibration* 279 (2005) 955–967.

[6] S. Chatterjee, A.K. Mallik, A. Ghosh, On impact dampers for non-linear vibrating systems, *Journal of Sound and Vibration* 187 (3) (1995) 403–420.

[7] A. Jonsson, J. Bathelt, G. Broman, Implications of modelling one-dimensional impact by using a spring and damper element, *Proceedings of the ImechE: Journal of Multi-body Dynamics* 219 (K) (2005) 299–305.